Kinetics and thermodynamics of adsorption of ionizable aromatic compounds from aqueous solutions by as-prepared and oxidized multiwalled carbon nanotubes

G.D. Sheng[a], D.D. Shao[a], X.M. Ren[a], X.Q. Wang[c], J.X. Li[a,b], Y.X. Chen[b], X.K. Wang[a,*]

[a] Key Laboratory of Novel Thin Film Solar Cells, Institute of Plasma Physics, Chinese Academy of Sciences, P.O. Box 1126, 230031 Hefei, PR China
[b] School of Nuclear Science and Engineering, North China Electric Power University, Beijing 102206, PR China
[c] Key Laboratory of Ion Beam Bioengineering, Institute of Plasma Physics, Chinese Academy of Sciences, P.O. Box 1126, 230031 Hefei, PR China

ARTICLE INFO

ABSTRACT

The adsorption of 1-naphthylamine, 1-naphthol and phenol on as-prepared and oxidized multiwalled carbon nanotubes (MWCNTs) has been investigated. The results illustrated that both as-prepared and oxidized MWCNTs showed high adsorption capacity for the three ionizable aromatic compounds (IACs) studied. Oxidation of MWCNTs increased the surface area and the pore volume, and introduced oxygen-containing functional groups to the surfaces of MWCNTs, which depressed the adsorption of IACs on MWCNTs. Both Langmuir and Freundlich models described the adsorption isotherms very well and the adsorption thermodynamic parameters (ΔG°, ΔH° and ΔS°) were measured. The adsorption for 1-naphthylamine, 1-naphthol and phenol is general spontaneous and thermodynamically favorable. The adsorption of phenol is an exothermic process, whereas the adsorption of 1-naphthylamine and 1-naphthol is an endothermic process. Results of this work are of great significance for the environmental application of MWCNTs for the removal of IACs from large volume of aqueous solutions.

© 2010 Elsevier B.V. All rights reserved.

1. Introduction

Since the discovery by Iijima in 1991 [1,2], carbon nanotubes (CNTs) have attracted great attention in multidisciplinary areas due to their unique hollow tube structure and their many outstanding mechanical, electronic and optical properties [3,4]. CNTs have been proposed for various applications such as hydrogen storage devices, sensors and so on [5,6]. Because of their large surface area and high reactivity, extensive experiments have been conducted on the adsorption of inorganic or organic contaminants on CNTs [7,8]. Lu et al. [9,10] investigated the adsorption–desorption of Zn^{2+} and Ni^{2+} on CNTs, and found that CNTs possessed higher adsorption capacity than granular activated carbon. It has also been demonstrated that CNTs are promising adsorbents for the removal of organic contaminants such as trihalomethanes [11,12], 1,2-dichlorobenzene [13], resorcinol [14], and polycyclic aromatic hydrocarbons [15–17] from aqueous solution. The adsorption of CNTs can be modified by oxidation using $KMnO_4$, H_2O_2, NaOCl or HNO_3 [13,18–20] as oxidant. Such oxidation can remove impurities of CNTs, which increases the surface area and introduces oxygen-containing functional groups

[20], thus altering the adsorption for environmental contaminants [12,13,18,19].

Ionizable aromatic compounds (IACs) such as hydroxyl- and amino-substituted aromatics are widely found in the effluents from pharmaceuticals, petrochemicals, dyestuffs, pesticides and other industries [21]. Many of them have been classified as hazardous pollutants because of their potential harmful to human health [21]. Due to their relatively high solubility in water, they can transport favorably in natural environment. For the removal of IACs from water, many studies have been focused on their adsorption by adsorbents and elucidating the mechanism of the adsorption process [21,22]. It was recently reported [22] that CNTs have stronger affinity for IACs than that for nonionic aromatic compounds. Since the oxidation of CNTs introduces oxygen-containing functional groups, it is possible that this would decrease the adsorption of organic compounds. However, the exact role of these oxygen-containing functional groups on the specific adsorption of IACs on CNTs is not clear.

Understanding the kinetic and thermodynamic of the adsorption is critical for the development of more efficient adsorbents suitable for real environmental applications. While studies of the adsorption kinetics and thermodynamics of heavy metals on MWC-NTs are generally well known, very little information is currently available regarding the adsorption of organic compounds, such

* Corresponding author. Tel.: +86 551 5592788; fax: +86 551 5591310.
  E-mail address: xkwang@ipp.ac.cn (X.K. Wang).

as trihalomethanes [11], 1,2-dichlorobenzene [12], atrazine [23], nitroaromatic compounds [23] and dyes [25,26] on MWCNTs. These limited studies suggested that the adsorption of organic compounds on MWCNTs was spontaneous and mainly due to physical adsorption.

In this work, the adsorption kinetics and thermodynamics of IACs on MWCNTs were studied. 1-naphthylamine, 1-naphthol and phenol were selected as model IACs because of their extensive existence in water environment. The aim of this work was to understand the kinetic and thermodynamic behavior of IACs adsorption on MWCNTs, and to reveal the effect of oxygen-containing functional groups on the adsorption of IACs on MWCNTs.

2. Materials and methods

2.1. Preparation and oxidation of MWCNTs

MWCNTs were prepared by using chemical vapor deposition (CVD) of acetylene in hydrogen flow at 760 °C using Ni–Fe nanoparticles as catalysts [27]. $Fe(NO_3)_2$ and $Ni(NO_3)_2$ were treated by the sol–gel process and calcinations to obtain FeO and NiO and then deoxidized by H_2 to achieve Fe and Ni nanoparticles. Oxidized MWCNTs were prepared by oxidization with 3 mol/L HNO_3 [28]. Briefly, 400 mL 3 mol/L HNO_3 including 2 g of MWCNTs was ultrasonically stirred for 24 h, filtrated, and then rinsed with doubly distilled water until the pH reached about 6. Such prepared sample was dried overnight in an oven at 80 °C, and then calcined at 450 °C for 4 h to completely remove amorphous carbon and nitrate ions [29]. The catalysts Fe and Ni in the oxidized MWCNTs were measured by ICP-MS and the results indicated that Ni and Fe were less than 0.01% and 0.03%, respectively.
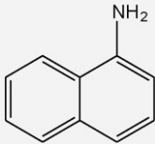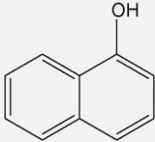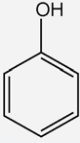
2.2. Chemicals

1-Naphthylamine, 1-naphthol and phenol were purchased from Guoyao Chemical Reagent Corporation (China). No significant impurities were detected by HPLC-UV analysis. Selected properties of 1-naphthylamine, 1-naphthol and phenol are listed in Table 1. The adsorbates were dissolved in 0.01 mol/L NaCl and 100 mg/L NaN_3 solution which were applied as support electrolyte (the pH was approximately 6.5) throughout this study. The final concentrations of the adsorbates were limited to <50% of their water solubility to ensure complete dissolution. All chemicals were purchased in analytical purity and used without further purification. Milli-Q water was used in all experiments.

2.3. Characterization

The morphology of MWCNTs was characterized by a field emission scanning electron microscope (FE-SEM, JEOL JSM-6700, Tokyo, Japan) and a high-resolution transmission electron microscope (HR-TEM, JEOL JEM-2010, Tokyo, Japan). The thermal stability of MWCNTs in air was determined by a thermogravimetric analyzer (Pyris 1 TGA, PerkinElmer, MA, USA) at a heating rate of 10 °C/min in temperature range of 30–800 °C. Fourier transform infrared (FTIR) technique was used in the analysis of the chemical surface groups of the adsorbents. FTIR analysis was performed using a Nexus670 FTIR spectrometer (Thermo Nicolet, Madison) equipped with a KBr beam splitter (KBr, FTIR grade). Spectra were acquired in the 4000–400 cm^{-1} wavenumber with 4 cm^{-1} resolution. The background spectrum of KBr was also recorded at the same conditions. The structural information of MWCNTs was evaluated by a Raman Spectrometer (Model Nanofinder 30R, Tokyo Instruments Inc., Tokyo, Japan). The acidic and basic site concentrations of adsorbents were determined by Boehm titration method [31]. The titration was conducted by adding 200 mg of adsorbents into a 200 ml flask containing 100 ml of the following 0.1 mol/L solutions: $NaHCO_3$, Na_2CO_3, NaOH, and HCl. The flask was sealed and shaken at 298 K for 2 days, and then filtered through a 0.45 mm nylon fiber filter. The filtrate (10 ml) was pipetted and mixed with 15 ml of 0.1 mol/L HCl or NaOH. The excess of acid and base was titrated with 0.1 mol/L NaOH and HCl, respectively. The quantities of acidity of various types were determined from the assumption that $NaHCO_3$ reacts with carboxylic groups, Na_2CO_3 reacts with carboxylic and lactonic groups, and NaOH reacts with carboxylic, lactonic and phenolic groups. The total basicity was determined from the amount of HCl reacted with the adsorbents [32].

Table 1
Chemical structures and selected properties of IACs applied in this study.[a]

IACs	Chemical structures	M	S	K_{ow}	BP	MP	pK_a
1-Naphthylamine		143.2	1704	501	573	323	3.92
1-Naphthol		144.2	866	501	555	328	9.34
Phenol		94.1	89,100	30	439	282	9.92

M: molecular weight, g/mol; S: aqueous solubility, mg/L; K_{ow}: octanol–water partition coefficient; MP and BP are melting and boiling point temperature (unit is K), respectively. pK_a: acid dissociation constant.

[a] Refs. [22,30].

2.4. Analytical methods

The adsorbate concentrations in the initial and final aqueous solutions were measured by using UV–vis spectrophotometer at 320 nm for 1-naphthylamine, at 332 nm for 1-naphthol and at 275 nm for phenol, respectively. In order to further enhance determination sensitivity, the analyzed solution was basified to a pH of 12 with 0.1 mol/L NaOH to make sure the solute present in dissociation state in solution, and the limit of detection were 0.1, 0.1, and 0.05 mg/L for 1-naphthylamine, 1-naphthol and phenol, respectively.

2.5. Kinetic experiments

Kinetic experiments were performed in 100 mL glass vials sealed with Teflon-lined screw caps at 298 K. Initially, MWCNTs (100 mg for 1-naphthylamine and 1-naphthol, 200 mg for phenol) were introduced to the supporting solution of 0.01 mol/L NaCl containing 100 mg/L NaN$_3$ solution and prior to the introduction of IACs, the vials were rotated for 24 h to hydrate the MWCNTs. The initial concentration was 50 mg/L for each IAC investigated. After the introduction of the IACs, samples were shaken for a certain time intervals, filtered through 0.45 μm cellulose acetate membrane filter, and analyzed for the equilibrium solution concentration of IACs. The quantity of IACs adsorbed at time t (min), q_t (mg/g), was deduced from the mass difference between initial ($t = 0$ min) and final solution concentration taken at time t (min).

2.6. Adsorption experiments

Adsorption experiments were carried out in 8 mL amber EPA vials equipped with Teflon-lined screw caps using a batch technique. Duplicate samples were done for each adsorption isotherm data point, and triplicate samples were done for each pH effect data point. For adsorption isotherm experiments, the range of chemical concentration studied was 10–100 mg/L and the pH for 1-naphthylamine, 1-naphthol and phenol was between 6.0 and 6.5 (measured at the end of batch adsorption), within these pH ranges, 1-naphthylamine, 1-naphthol and phenol existed mainly in neutral form. For the pH effect experiments, the initial concentration was 50 mg/L for each IAC and the equilibrium pH was set over a range of 3–11. Prior to initiating an adsorption experiment, a certain amount of MWCNTs (8 mg for 1-naphthylamine and 1-naphthol, 16 mg for phenol) was transferred to a 8 mL vial and was equilibrated for 24 h with a certain volume of electrolyte solution containing 0.01 mol/L NaCl and 100 mg/L NaN$_3$ solution (as the bioinhibitor), the pH of the background solution was approximately 6.5. Afterward, a stock solution of an adsorbate (in methanol) was added to the vial using a microsyringe, the volume percentage of the methanol stock solution was kept below 0.1% (v/v) to minimize the cosolvent effect. The vial was then filled with an electrolyte solution to leave minimal head space and was mixed end over end at 3 rpm with a tumbler at room temperature for more than 3 days. The time required to reach adsorption equilibrium was predetermined by the kinetic experiments. After reaching equilibrium, the vials were removed from the tumbler and were left undisturbed on a flat surface for more than 24 h to allow complete settlement of MWCNTs. Aliquots of the aqueous solution were then withdrawn from the vials and filtered through 0.45 μm cellulose acetate membrane filter, and analyzed for the equilibrium concentration of adsorbates. Blank experiments were performed using the same experimental procedure but without MWCNTs to check for potential adsorption of IACs to the vials or the membrane filters, which could potentially result in nonspecific loss and/or degradation of the IACs. Such losses in the blank experiments were less than 5% of the initial concentrations and therefore indicated that the losses were small and can be

negligible. The amount of IACs adsorbed by MWCNTs could be calculated directly from mass difference between the initial and final equilibrium concentrations using Eq. (1):

$$q_e = \frac{(C_0 - C_e) \times V}{m} \tag{1}$$

where q_e is adsorbed amounts by MWCNTs (mg/g) after equilibrium, C_0 is the initial concentration (mg/L), C_e is the equilibrium concentration (mg/L), V is the solution volume (mL), and m is the MWCNTs dosage (g).

2.7. Data analysis

2.7.1. Kinetic study

For kinetic study, four common kinetic models including (1) pseudo-second-order model, (2) parabolic diffusion model, (3) Elovich model, and (4) modified Freundlich model have been tested for goodness of fit for the experimental data using the correlation coefficient (R) as a measure of the agreement between the experimental data and the four proposed models. Each of the models is briefly discussed below.

The pseudo-second-order model consists of all the steps of adsorption including external film diffusion, adsorption, and internal particle diffusion, which can be written as [24]:

$$\frac{dq_t}{dt} = k_2(q_e - q_t)^2 \tag{2}$$

where k_2 [g/(mg h)] is the rate constant of the pseudo-second-order adsorption, and is a complex function of the initial concentration of solute [24], and q_e and q_t are the adsorbed IACs (mg/g) at equilibrium and at time t (h). Given that the initial sorption rate v_0 [mg/(g h)] is:

$$v_0 = k_2 q_e^2 \tag{3}$$

Eq. (2) can be rearranged to give the linear expression:

$$\frac{t}{q_t} = \frac{1}{v_0} + \frac{1}{q_e}t \tag{4}$$

Thus the values of v_0 and k_2 can be determined experimentally by plotting t/q_t versus t and extracting information from the least-squares analysis of slope and intercept and substituting into Eq. (3).

The parabolic diffusion model can be used to determine whether diffusion-controlled phenomena are a rate-limiting step during adsorption [24]. The parabolic diffusion model can be written as:

$$\frac{q_t}{q_e t} = kt^{0.5} + a \tag{5}$$

where q_e and q_t are the adsorbed IACs (mg/g) at equilibrium and at time t (min), a is a constant, and k is the overall diffusion constant for adsorption.

The Elovich model can be written as [24]:

$$q_t = a \ln(t) + b \tag{6}$$

where q_t is the adsorbed IACs (mg/g) at time t (min), and a and b are constants whose chemical significance is not clearly defined.

The modified Freundlich model can be written as [24]:

$$q_t = kc_0 t^a \tag{7}$$

where q_t is the adsorbed IACs (mg/g) at time t (min), k is the rate constant for the sorption, a is a constant.

2.7.2. Isotherm modeling

In this study, both the Langmuir and the Freundlich models were employed to fit the experimental data.
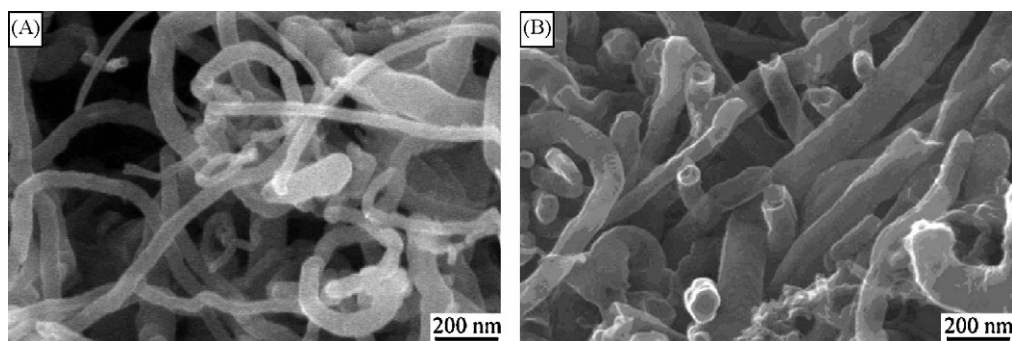
Fig. 1. Scanning electron microscope (SEM) images of as-prepared (A) and oxidized (B) MWCNTs.

The form of the Langmuir isotherm can be represented by the following equation [35]:

$$q_e = \frac{bq_{max} C_e}{1 + bC_e} \qquad (8)$$

Eq. (8) can be expressed in linear form:

$$\frac{1}{q_e} = \frac{1}{q_{max}} + \frac{1}{bq_{max}} \cdot \frac{1}{C_e} \qquad (9)$$

where q_{max} and b are Langmuir constants related to adsorption capacity and adsorption energy, respectively.

The Freundlich isotherm model has the following form [36]:

$$q_e = k_F C_e^n \qquad (10)$$

Eq. (10) can be expressed in linear form:

$$\log q_e = \log k_F + n \log C_e \qquad (11)$$

where k_F (mg^{1-n} g^{-1} L^n) represents the adsorption capacity when adsorbate equilibrium concentration equals to 1, and n represents the degree of adsorption dependence at equilibrium concentration.

Both the standard coefficient of determination (R^2) and the adjusted coefficient of determination (R^2_{adj}) were employed to compare the goodness of fitting between model prediction and measured data. The R^2_{adj} was calculated as [37]:

$$R^2_{adj} = \frac{1 - R^2(m - b)}{m^2 - 1} \qquad (12)$$

where m is the number of data points used for fitting, and b is the number of coefficients in the fitting equation.

2.7.3. Thermodynamic study

The measurement of the thermodynamic parameters, such as the adsorption equilibrium constant (K_0), the standard free energy changes ($\Delta G°$), the standard enthalpy change ($\Delta H°$) and the standard entropy change ($\Delta S°$) has been the subject of adsorption process. The distribution adsorption coefficient, K_d, is calculated from the following equation:

$$K_d = \frac{C_0 - C_e}{C_e} \cdot \frac{V}{m} \qquad (13)$$

where C_0 is the initial concentration (mg/L), C_e is the equilibration concentration after centrifugation (mg/L), V is the volume (mL) and m is the mass of adsorbent (g). Therefore, the adsorption equilibrium constant, K_0, can be calculated by plotting $\ln K_d$ versus C_e and extrapolating C_e to zero; the value of the intercept is the value of $\ln K_0$.

The standard free energy change ($\Delta G°$) can be calculated from the relationship:

$$\Delta G^0 = -RT \ln K_0 \qquad (14)$$

where R is the universal gas constant (8.314 J mol^{-1} K^{-1}), T is the temperature in Kelvin. The standard enthalpy change ($\Delta H°$) and the standard entropy change ($\Delta S°$) are calculated:

$$RT \ln K_0 = T\Delta S^0 - \Delta H^0 \qquad (15)$$

$$\ln K_0 = \frac{\Delta S^0}{R} - \frac{\Delta H^0}{RT} \qquad (16)$$

The values of $\Delta H°$ and $\Delta S°$ can be calculated from the slope and y-intercept of the plot of $\ln K_d$ versus $1/T$ by using Eq. (16).

3. Results and discussion

3.1. Characterization of MWCNTs

Fig. 1A and B displays the SEM images of as-prepared and oxidized MWCNTs, respectively. It is evident that the isolated MWCNTs usually curve and have cylindrical shapes with the
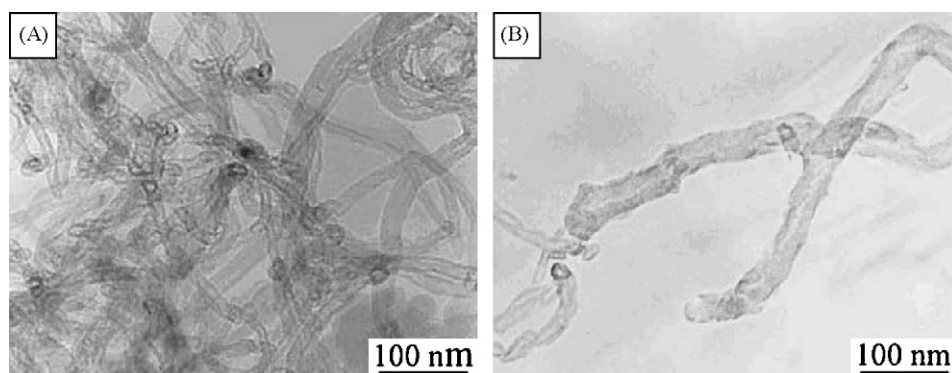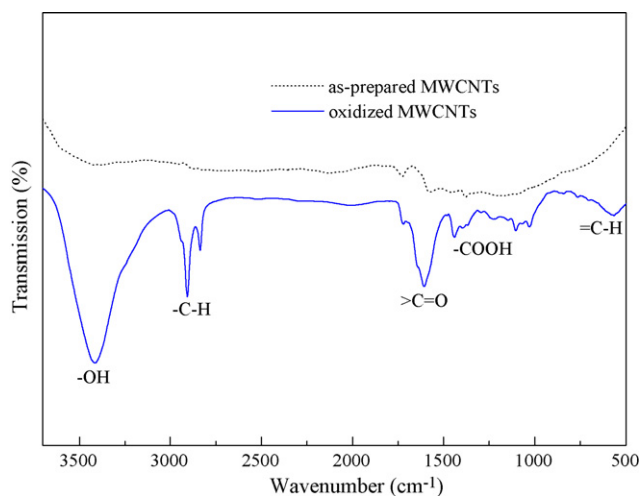

Fig. 2. Transmission electron microscope (TEM) images of as-prepared (A) and oxidized (B) MWCNTs.
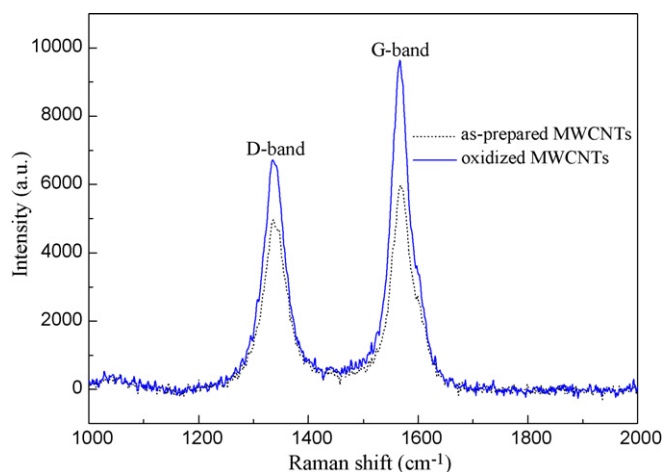
Fig. 3. Fourier transformation infrared (FTIR) spectra of as-prepared and oxidized MWCNTs.

Fig. 5. Thermo gravimetric analysis–differential thermal analysis (TGA–DTA) curves of as-prepared and oxidized MWCNTs.

diameter range of 10–30 nm for MWCNTs, respectively. Due to inter-molecular force, the isolated MWCNTs of different size and direction can form an aggregated structure. The length of MWCNTs becomes short and the confined space among isolated MWCNTs becomes small after oxidation.
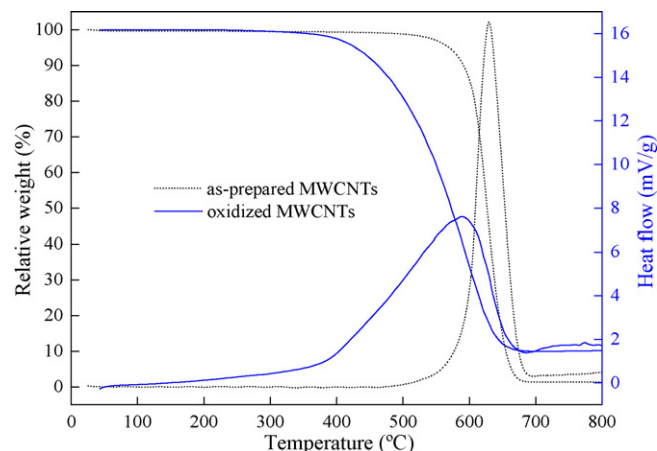
Fig. 2A and B shows the TEM images of as-prepared and oxidized MWCNTs, respectively. As can be seen, a large amount of metal catalysts and amorphous carbon appeared within as-prepared MWCNTs and was removed after oxidation. TEM images of MWCNTs contain a concentrically nested array of SWCNTs with the hollow inner tube diameter of around 10 nm.

The FTIR measurements were performed in order to verify the formation of oxygen-containing functional groups after oxidation. Fig. 3 shows the FTIR spectra of as-prepared and oxidized MWC-NTs. It is clear that the spectra of MWCNTs display no significant bands before the oxidation but show some apparent bands after oxidation. The FTIR spectra indicate that the acid treatment process introduces many functional groups on the surfaces of MWCNTs: carbonyl groups (1400 cm^{-1}), carboxyl groups (1650 cm^{-1}), and hydroxyl groups (3500 cm^{-1}). These functional groups are produced abundantly on the external and internal surface of oxidized MWCNTs, which increase the surface polarity and further alter the surface charges.

The Raman spectra of as-prepared and oxidized MWCNTs in Fig. 4 are composed of two characteristic peaks. The peak

Fig. 4. Raman spectra of as-prepared and oxidized MWCNTs.

near 1350 cm^{-1} is the D-band corresponding to the disordered sp^2-hybridized carbon atoms of MWCNTs while the peak near 1580 cm^{-1} is the G-band corresponding to the structural integrity of sp^2-hybridized carbon atoms of MWCNTs. Together, these bands can be used to determine the extent of carbon-containing defects [38]. As can be seen, the as-prepared MWCNTs ($I_D/I_G = 0.85$) have a higher I_D/I_G ratio (the intensity ratio of D-band to G-band) than the oxidized MWCNTs ($I_D/I_G = 0.79$), which indicates that the as-prepared MWCNTs contain more amorphous carbon and multishell sp^2-hybridized carbon nanoparticles [39].

Fig. 5 reveals the TGA–DTA results of as-prepared and oxidized MWCNTs. It is evident that the as-prepared MWCNTs are considerably stable and show a little weight loss close to 5.2% below 500 °C. A significant gasification of MWCNTs begins at 500 °C and ends at 610 °C, in which 7.25% remaining weight is found. The oxidized MWCNTs have a broader temperature range for weight loss than that of the as-prepared MWCNTs and exhibit three main weight loss regions, which can be attributed to the removal of amorphous carbons and metal catalysts after oxidation as shown in SEM and TEM images. Similar TGA–DTA results have been reported for as-prepared and functionalized MWCNTs [38] (Table 2).

The results of Boehm titration are shown in Table 3. It is obvious that the total acidity of MWCNTs increased after oxidation, which can be caused by the presence of more carboxyls, lactones or phenols on the MWCNT walls. Carboxylic groups are the major acidity, followed by lactonic groups, and then phenolic groups. The total basicity of MWCNTs also increased after oxidation, which may be caused by the presence of more oxygen functional groups and the existence of pyrone-type structures on the edges of the polyaromatic layers [32]. However, the origin of surface basicity after oxidation of MWCNTs is still under discussion and further studies are needed.

3.2. Adsorption kinetics

Fig. 6 demonstrates the adsorption kinetics of IACs on as-prepared and oxidized MWCNTs. The plots represent the adsorbed IACs on as-prepared and oxidized MWCNTs versus time at an initial concentration of 50 mg/L. For the three IACs studied in this work, the adsorption was very fast on both as-prepared and oxidized MWCNTs. Apparent equilibrium was reached within 5 h, this fast adsorption process was quite similar to that which had been reported for trihalomethanes [11], reactive dyes [25] and nitroaromatic compounds [24]. Individual MWCNTs have a dominant adsorption domain which is primarily the outermost graphene surface and defect sites. However, when MWCNTs form bundles in

Table 2
Selected properties of as-prepared and oxidized MWCNTs applied in this study.

MWCNTs	Specific surface area (m^2/g)[a] BET method	Micropore volume (cm^3/g)[a] t-plot method	2–100 nm pore volume (cm^3/g)[a] BJH method	C (%)[b]	H (%)[b]	O (%)[c]	pH_{pzc}[d]
As-prepared	72	0.008	0.41	93.0	0.26	2.76	~5.5
Oxidized	121	0.0004	0.49	90.0	0.19	8.50	<5.0

[a] Ref. [14].
[b] Ref. [24].
[c] Ref. [33].
[d] Ref. [34].

Table 3
Results of Boehm titration of as-prepared and oxidized MWCNTs.

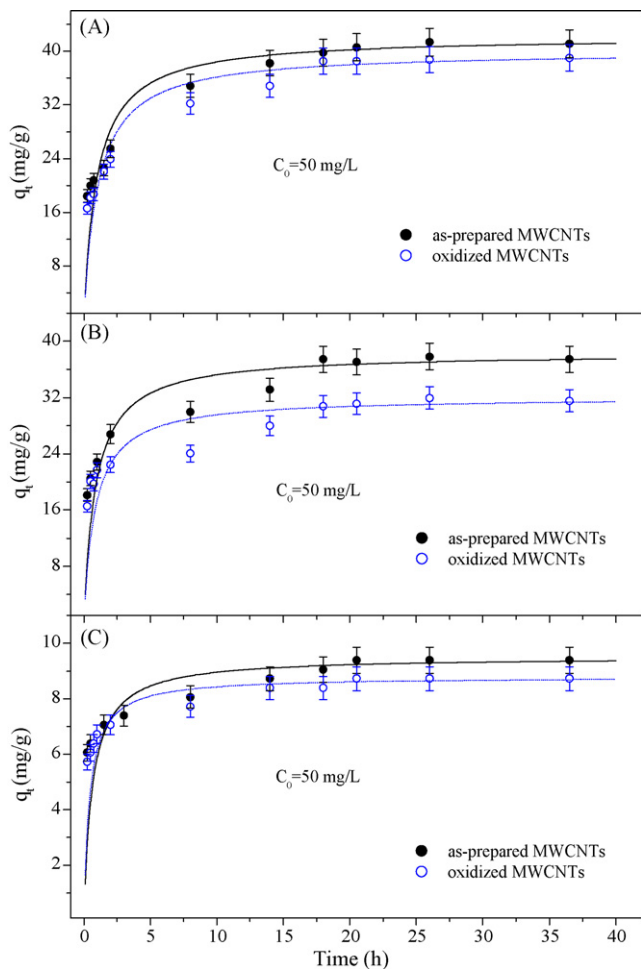| MWCNTs	Carboxylic groups	Lactone groups	Phenolic groups	Total acidity	Total basicity
As-prepared	0.65	0.28	0.55	1.48	0.10
Oxidized	1.10	0.34	0.68	2.12	0.15

aqueous media, the interstitial channel space between the tubes within the bundles can be regarded as pores [24]. Therefore, IACs were thought to preferentially occupy the external graphene surface of MWCNTs during the initial adsorption process, while the overall adsorption of IACs included the contributions from the adsorption on the graphene surface as well as due to pore filling.

While four kinetic models, pseudo-second-order model, parabolic diffusion model, modified Freundlich model, and Elovich model, were applied to simulate the experimental data, and only

Fig. 6. Adsorption kinetics of 1-naphthylamine (A), 1-naphthol (B) and phenol (C) onto as-prepared and oxidized MWCNTs at an initial concentration of 50 mg/L. Lines represent the model fitting of pseudo-second-order equation.

the pseudo-second-order model fitted the adsorption kinetics well with correlation coefficient consistently >0.999 for all three IACs studied (Table 3). The other three kinetic models failed to describe the experimental data well, as indicated by consistently lower R values (data not shown). Shen et al. [24] studied the adsorption kinetic of four nitroaromatic compounds on as-prepared and oxidized MWCNTs, and similar results have been reported. The initial adsorption rate (v_0) and the adsorption rate constant (q_e) of the oxidized MWCNTs were both smaller than those of the as-prepared MWCNTs, suggesting that the adsorption of IACs on as-prepared MWCNTs was faster than that on the oxidized MWCNTs (Table 4). The difference in adsorption kinetics between as-prepared and oxidized MWCNTs may be due to the changes in the surface chemistry of MWCNTs after HNO_3 oxidization. After oxidization, hydrophilic oxygen-containing groups, including carboxylic, lactonic, and hydroxyl groups, were introduced into the outmost surface and defect sites of MWCNTs. The addition of these groups results in a more negatively charged MWCNT surface due to deprotonation of carboxylic groups at the equilibrium adsorption pH of 6.5, since at this pH the adsorption of water is more energetically favorable relative to the adsorption of IACs and thus the adsorption of IACs becomes more difficult.

3.3. Effect of pH

For organic acids and organic bases, the occurrence of their nondissociated or dissociated species depends on the solution pH in relation to their dissociated constants (pK_a). When pH < pK_a, the nondissociated species and the dissociated species are dominated for organic acids and organic bases, respectively; whereas, when pH > pK_a, the dissociated species (anion) is dominant for organic acids and the nondissociated species is dominant for organic bases. The fraction of nondissociated species for organic acids (f_A^N) and bases (f_B^N) can be respectively estimated by $f_A^N = (1 + 10^{pH-pK_a})^{-1}$ and $f_B^N = (1 + 10^{pK_a-pH})^{-1}$, and the fraction of dissociated species for organic acids (f_A^I) and bases (f_B^I) can be estimated by $f_A^I =$

Table 4
Kinetic parameters of pseudo-second-order model fitting for IACs adsorption on as-prepared and oxidized MWCNTs.

MWCNTs	IACs	v_0	q_e	R^2
As-prepared	1-Naphthylamine	14.43	8.80	0.999
	1-Naphthol	43.86	38.31	0.997
	Phenol	15.30	9.51	0.999
Oxidized	1-Naphthylamine	37.59	40.00	0.999
	1-Naphthol	37.88	32.05	0.996
	Phenol	52.327	10.551	0.999
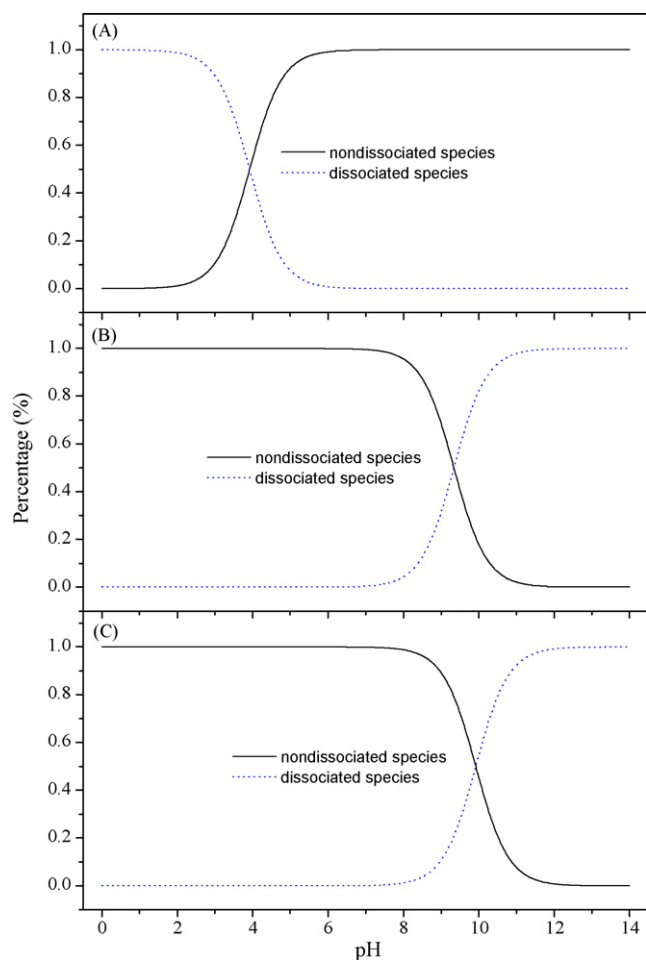
Fig. 7. Species distribution of 1-naphthylamine (A), 1-naphthol (B) and phenol (C) as a function of pH values.

Fig. 8. Adsorption of 1-naphthylamine (A), 1-naphthol (B) and phenol (C) on as-prepared and oxidized MWCNTs as a function of pH values.

$(1 + 10^{pK_a-pH})^{-1}$ and $f_B^I = (1 + 10^{pH-pK_a})^{-1}$, respectively [41]. Fig. 7 shows the distribution of their nondissociated or dissociated species as a function of pH values for 1-naphthylamine, 1-naphthol and phenol, respectively.

Fig. 8 demonstrates that the pH effect on adsorption varied for different chemicals studied in this work. Changing the pH over the range of 3–11 should have significantly affected the protonation–deprotonation transition of MWCNT surface groups such as –OH and –COOH, and it appears that such a transition has significant effect on the adsorptive affinity of IACs. The effect of pH on the adsorption of phenol was insignificant when the pH was below the phenol's pK_a (9.92), but the adsorption was considerably hindered when the pH was above the pK_a. Moreover, this pH effect was more significant for the adsorption to oxidized MWCNTs than to as-prepared MWCNTs. Lin and Xing [40] and Yang et al. [41] have studied the pH effect on the adsorption of phenolic compounds by MWCNTs, respectively, and similar results were reported. Surprisingly, when the pH was below its pK_a (9.34), the adsorption of 1-naphthol increased with the pH, and the trend was also much more significant for the adsorption to oxidized MWCNTs than to as-prepared MWCNTs. However, when the pH was above the pK_a, different trends were observed on the different adsorbents: adsorption to as-prepared MWCNTs was similar to that at pH 8 and 9 but stronger than that at the lower pH values; adsorption to oxidized MWCNTs was weaker at pH 11 than at pH 8 but still considerably stronger than that at the lower pH values. For 1-naphthylamine, the adsorption to oxidized MWCNTs increased by over 1 order of magnitude over the pH range of 3–7 but slightly decreased when the pH
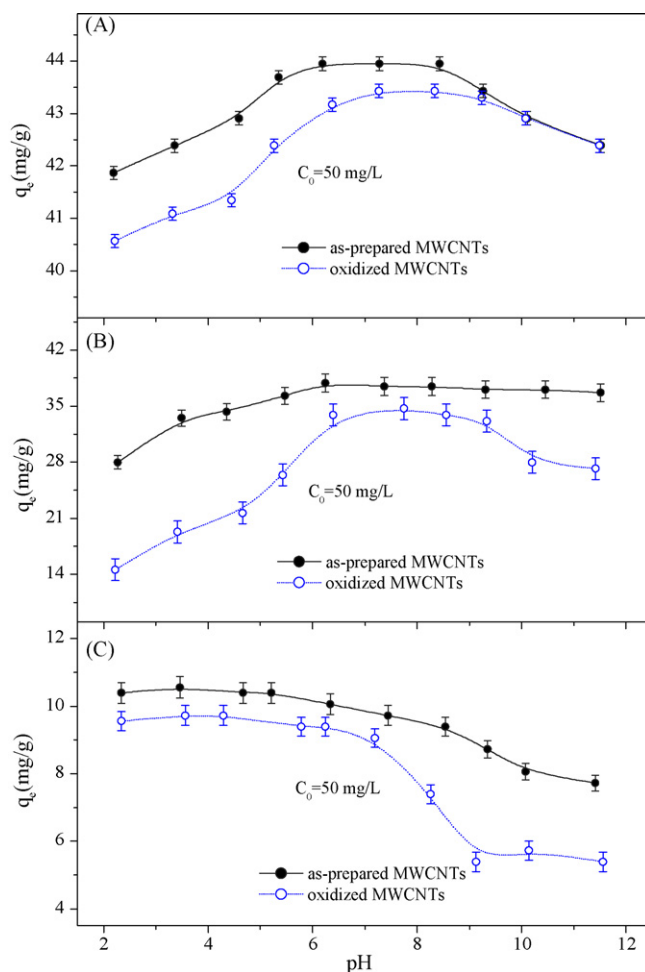
further increased. A similar trend of the pH effect was observed on as-prepared MWCNTs when the pH was less than 9, but the adsorption affinity decreased with the pH pronouncedly at higher pH values. Chen et al. [22] have investigated the effect of pH on adsorption of MWCNTs for 1-naphthol and 1-naphthylamine, respectively, and similar observation was also found.

3.4. Comparison of as-prepared and oxidized MWCNTs

It has been reported that oxidized MWCNTs became more hydrophilic and suitable for the adsorption of trihalomethanes than as-prepared MWCNTs [12]. Herein, we compared the adsorption ability of as-prepared MWCNTs with that of oxidized MWCNTs. Fig. 9A illustrates the adsorption of 1-naphthylamine on as-prepared and oxidized MWCNTs, respectively. Two curves resemble the same trend; however, the adsorption for oxidized MWCNTs is much lower than that for as-prepared MWCNTs. Similar results are also observed for the 1-naphthol and phenol adsorption.

The oxidation process alters the surface properties of MWCNTs from two aspects. On the one hand, MWCNTs become more hydrophilic and have more active functional groups on the surfaces. On the other hand, the physical properties such as the specific surface area and pore volume distribution are changed significantly. As it has been discussed above, the adsorption of 1-naphthylamine on MWCNTs is not dependent on the porous structure, which is supported by the recent work of Yang et al. [16] with regard to the competitive adsorption of pyrene, phenanthrene, and naphthalene
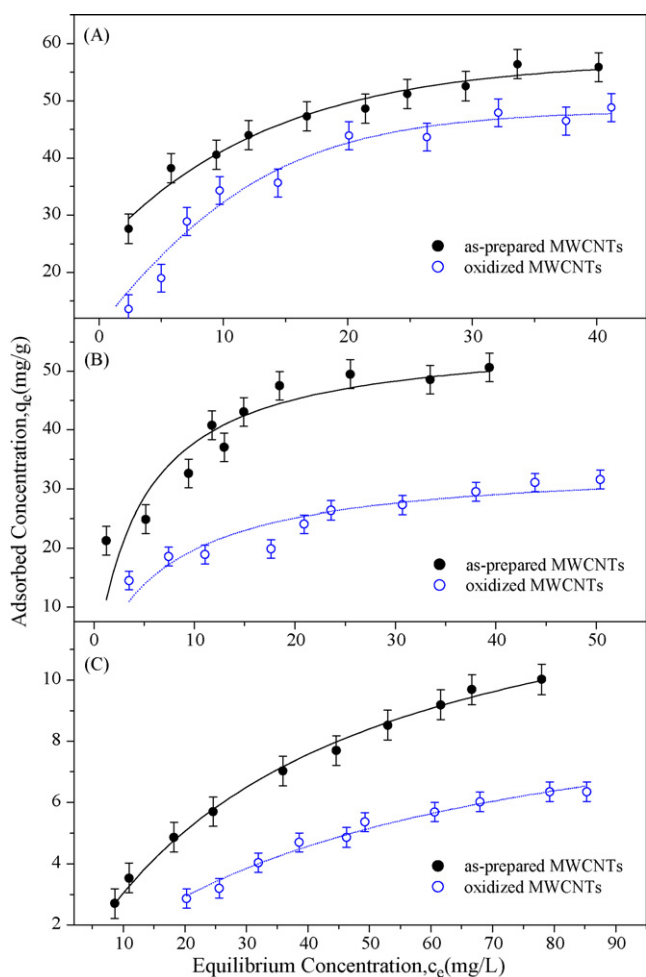
Fig. 9. Adsorption isotherms of 1-naphthylamine (A), 1-naphthol (B) and phenol (C) on as-prepared and oxidized MWCNTs, respectively.

on MWCNTs. The results of the lower adsorption for HNO$_3$-oxidized MWCNTs also indicate that surface chemical properties rather than specific surface areas or pore volume are important factors to determine the adsorption of MWCNTs. The oxidization of MWCNTs by HNO$_3$ or H$_2$SO$_4$/HNO$_3$ mixture introduced carboxylic groups [42], which made the surface of MWCNTs negatively charged. The surface modified MWCNTs may inhibit adsorption of IACs on MWCNTs due to repulsion of negative charges. Moreover, carboxylic groups on the surfaces of oxidized MWCNTs can act as electrons withdrawing groups localizing electron from π system of MWCNTs, which might be expected to interfere with π–π dispersion forces between the aromatic ring of IACs and the graphitic structure of MWCNTs. Numerous studies have shown that the oxygen functional groups depressed the adsorption of organic chemicals on carbon materials [43,44] by water adsorption, dispersive–repulsive interactions, and hydrogen bonding. Previous studies on the adsorption of aromatics on activated carbon suggested that surface oxygen complexes increased the affinity of water to activated carbon, which reduced the accessibility for aromatic adsorbates, thus led to the lower adsorption capacity [43,45]. This is another reason for the reduction of the adsorption capacity of oxidized MWCNTs.

3.5. Adsorption isotherms

The adsorption isotherm is the most important information, which indicates how adsorbate molecules are distributed between the liquid phase and solid phase when the adsorption process

reaches equilibrium. Fig. 10 presents the adsorption isotherms of 1-naphthylamine, 1-naphthol and phenol on as-prepared and oxidized MWCNTs at three different temperatures, respectively. The relative parameters derived from the Langmuir and Freundlich models are listed in Table 5. It can be seen from Table 5 that the experimental data of 1-naphthylamine, 1-naphthol and phenol adsorption are well fitted by both Langmuir and Freundlich models, which means physical adsorption occurred. Both as-prepared and oxidized MWCNTs have nonlinear adsorption isotherms for ionizable aromatic compounds studied in this work, due to the heterogeneous adsorption sites of MWCNTs. Because of its strong hydrophobicity, the isolated MWCNTs of different sizes can form aggregated structure as observed by SEM and TEM. Aggregation of MWCNTs may create heterogeneous sites with different adsorption energies for IACs adsorption. The heterogeneous sites of MWCNTs may stem from the following types: (i) in the hollow space inside nanotubes, (ii) in the interstitial spacing between neighboring nanotubes, (iii) on the grooves of the periphery of nanotube bundles, and (iv) on the curved surface of the periphery of nanotubes [46].

It is of great importance to disclose the adsorption mechanism of IACs on as-prepared and oxidized MWCNTs. It has been widely accepted that the strong adsorption of aromatic compounds on CNTs was mainly attributed to the π–π electron-donor–acceptor (EDA) interaction between aromatic molecules and the highly polarizable graphene sheets of CNTs [8,22,33,40]. Chen et al. [22] have proposed that the strong adsorptive interaction between hydroxyl-substituted aromatics and CNTs was mainly due to the electron-donating effect of the hydroxyl group, which caused a strong EDA interaction between the adsorbates and the π-electron-depleted regions on the graphene surfaces of CNTs. In addition to the EDA interaction, Lewis acid–base interaction was likely an extra important mechanism contributing to the strong adsorption of 1-naphthylamine, especially on the O-functionality-abundant carbon nanotubes. Furthermore, hydrogen bonding, hydrophobic effect, electrostatic interaction may another important factors that are responsible for the adsorption of IACs on MWCNTs.

3.6. Adsorption thermodynamics

To assess the thermodynamic parameters, the adsorption isotherms of 1-naphthylamine, 1-naphthol and phenol on as-prepared and oxidized MWCNTs were measured at 298, 318, and 338 K, respectively (Fig. 10). The distribution coefficients as a function of solute final concentration at 298, 318, and 338 K are shown in Fig. 11. The values of adsorption equilibrium constant ($\ln K_0$) are obtained by plotting $\ln K_d$ versus C_e and extrapolating C_e to zero; and the value of the intercept is the value of $\ln K_0$ (see Fig. 11). Constants of linear fit of $\ln K_d$ versus C_e for the adsorption of 1-naphthylamine, 1-naphthol and phenol on as-prepared and oxidized MWCNTs are listed in Table 6. The slope of Eq. (16) is $-\Delta H^\circ/R$ and the intercept is $\Delta S^\circ/R$ (see Fig. 12). Thermodynamic parameters calculated from Eqs. (14) and (16) are listed in Table 7. The evaluation of thermodynamic parameters provides an insight into the mechanism of IACs adsorption on as-prepared and oxidized MWCNTs.

Firstly, all the samples present a negative standard free energy change and a positive standard entropy change, which indicate that the adsorption reactions are general spontaneous process and thermodynamically favorable. The positive standard entropy changes indicate that the degree of freedom increases at the solid–liquid interface during the adsorption of IACs on MWCNTs. IACs in solution is surrounded by a tightly bound hydration layer where water molecules are more highly ordered than in the bulk water. When a molecule of IACs comes into close interaction with the hydration surface of MWCNTs, the ordered water molecules in these two hydration layers are compelled and disturbed, thus increas-
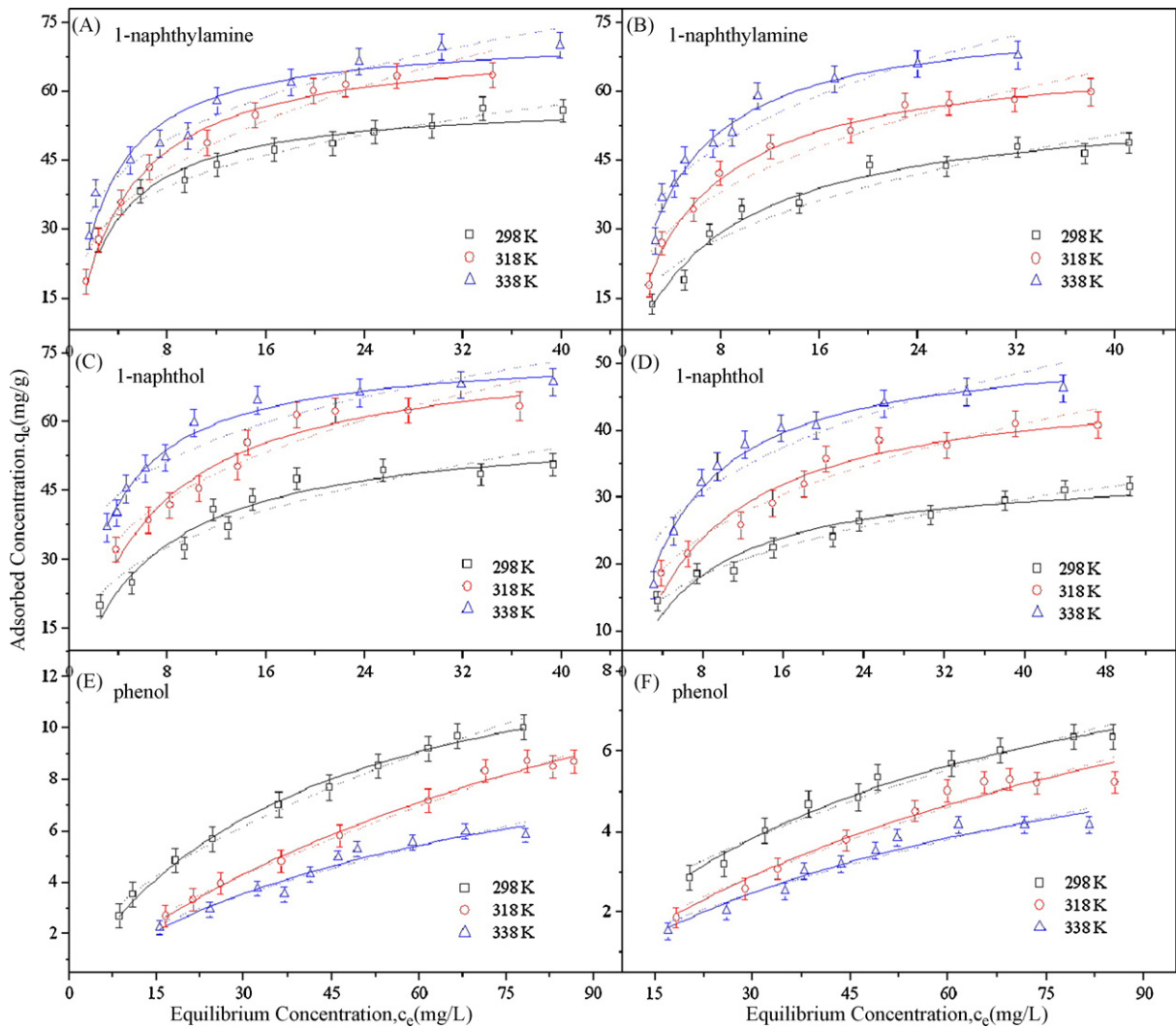
Fig. 10. Adsorption isotherms of IACs on as-prepared MWCNTs (A, C, E) and oxidized MWCNTs (B, D, F) at three different temperatures. Symbols denote experimental data, solid lines represent the model fitting of Langmuir equation, dotted lines represent the model fitting of Freundlich equation.

Table 5A
The parameters for Langmuir isotherms at three different temperatures.

MWCNTs	IACs	298 K				318 K				338 K			
		q_{max}	$1/b$	R^2	R^2_{adj}	q_{max}	$1/b$	R^2	R^2_{adj}	q_{max}	$1/b$	R^2	R^2_{adj}
As-prepared	1-Naphthylamine	58.82	2.69	0.97	0.92	72.46	3.89	0.98	0.92	83.33	2.63	0.94	0.93
	1-Naphthol	54.35	4.69	0.94	0.93	72.36	5.18	0.95	0.93	76.34	3.33	0.99	0.92
	Phenol	14.41	36.01	0.99	0.92	13.81	73.27	0.99	0.92	10.91	61.69	0.97	0.92
Oxidized	1-Naphthylamine	58.14	8.17	0.97	0.92	71.43	6.10	0.98	0.92	80.00	4.47	0.95	0.93
	1-Naphthol	30.58	43.10	0.91	0.93	43.10	5.55	0.93	0.93	57.80	3.10	0.98	0.92
	Phenol	11.26	59.85	0.98	0.92	10.64	92.12	0.91	0.93	10.17	97.12	0.98	0.92

Table 5B
The parameters for Freundlich isotherms at three different temperatures.

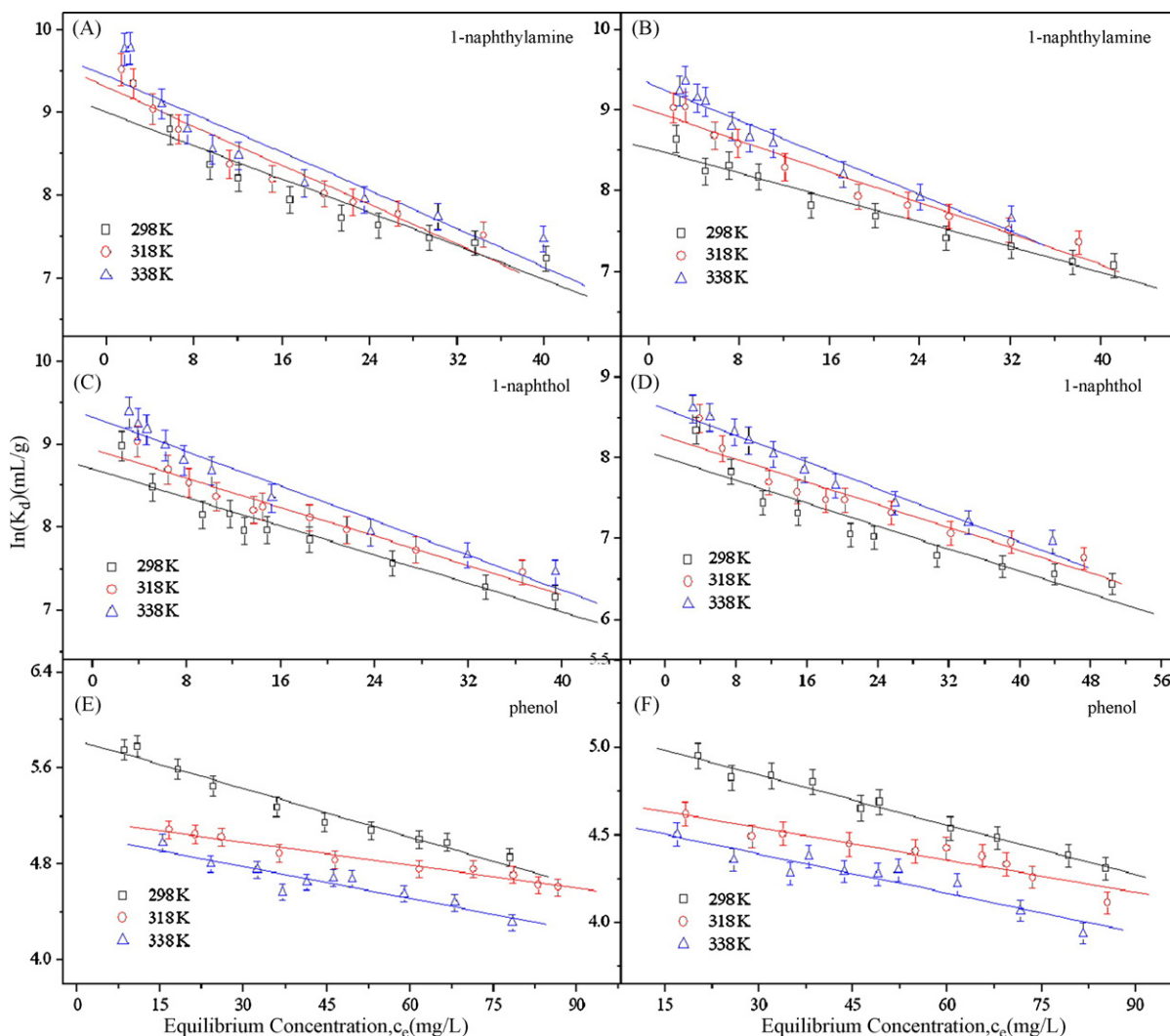| MWCNTs	IACs	298 K				318 K				338 K			
		k_F	n	R^2	R^2_{adj}	k_F	n	R^2	R^2_{adj}	k_F	n	R^2	R^2_{adj}
As-prepared	1-Naphthylamine	23.46	0.24	0.98	0.92	24.35	0.37	0.96	0.93	28.31	0.27	0.96	0.93
	1-Naphthol	14.84	0.36	0.93	0.93	21.00	0.34	0.94	0.93	30.73	0.24	0.91	0.93
	Phenol	0.86	0.58	0.99	0.92	0.91	0.72	0.99	0.92	0.81	0.65	0.96	0.93
Oxidized	1-Naphthylamine	10.57	0.44	0.93	0.93	24.36	0.33	0.90	0.94	16.31	0.39	0.93	0.93
	1-Naphthol	9.92	0.30	0.99	0.92	11.69	0.34	0.97	0.92	14.69	0.35	0.88	0.94
	Phenol	0.54	0.57	0.96	0.93	0.22	0.74	0.97	0.92	0.21	0.70	0.95	0.93

Fig. 11. Linear plots of $\ln K_d$ vs. C_e for the adsorption of IACs on as-prepared MWCNTs (A, C, E) and oxidized MWCNTs (B, D, F) at three different temperatures.

Table 6
Constants of linear fit of $\ln K_d$ vs. C_e ($\ln K_d = B + AC_e$).

MWCNTs	IACs	298 K			318 K			338 K		
		A	B	R	A	B	R	A	B	R
As-prepared	1-Naphthylamine	−0.05	9.01	0.88	−0.06	9.30	0.92	−0.06	9.44	0.86
	1-Naphthol	−0.04	8.70	0.91	−0.04	8.94	0.94	−0.05	9.33	0.95
	Phenol	−0.01	5.12	0.98	−0.01	4.73	0.89	−0.01	4.62	0.88
Oxidized	1-Naphthylamine	−0.04	8.52	0.96	−0.05	9.00	0.96	−0.06	9.33	0.95
	1-Naphthol	−0.04	8.00	0.87	−0.04	8.26	0.90	−0.04	8.61	0.96
	Phenol	−0.01	5.83	0.94	−0.01	5.17	0.97	−0.01	5.04	0.87

Table 7
Thermodynamic parameters of IACs adsorbed on as-prepared and oxidized MWCNTs.

MWCNTs	IACs	ΔG° (kJ mol^{-1})			ΔS° (J mol^{-1} K^{-1})	ΔH° (J mol^{-1})
		298 K	318 K	338 K		
As-prepared	1-Naphthylamine	−5.44	−5.90	−6.31	101.85	9.24
	1-Naphthol	−5.15	−5.58	−6.05	127.72	16.90
	Phenol	−4.37	−4.34	−4.56	116.43	−13.19
Oxidized	1-Naphthylamine	−5.31	−5.81	−6.28	108.61	12.59
	1-Naphthol	−4.37	−4.34	−4.55	8.02	16.64
	Phenol	−4.05	−4.10	−4.30	6.31	−10.72
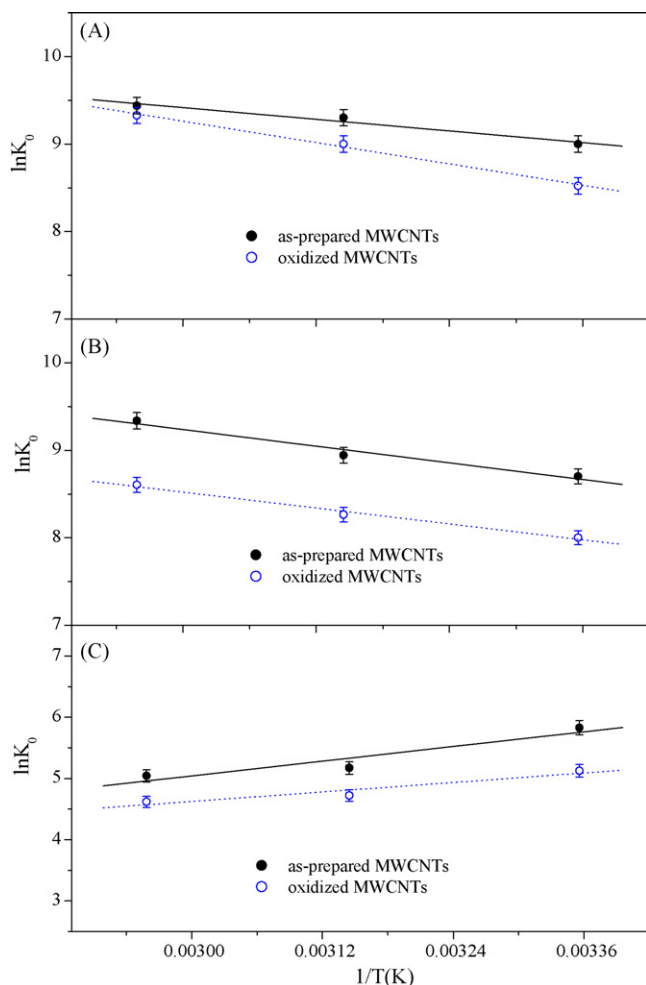
Fig. 12. Linear plots of $\ln K_0$ vs. $1/T$ for 1-naphthylamine (A), 1-naphthol (B) and phenol (C) adsorption on as-prepared and oxidized MWCNTs, respectively.

ing the entropy of water molecules. Although the adsorption of IACs molecules on MWCNTs decreases the degree of freedom of IACs molecules, it seems likely that positive entropy associated with the adsorption of IACs on MWCNTs is due to the entropy increase of water molecules overweighing the entropy decrease of IACs molecules.

Secondly, an interesting observation is that the average standard enthalpy changes are negative for phenol adsorption on as-prepared and oxidized MWCNTs while they are positive for 1-naphthylamine and 1-naphthol adsorption. The observed negative ΔH° values suggested an exothermic adsorption for phenol, which was supported by the observation that adsorption of phenol on as-prepared and oxidized MWCNTs decreased with increasing adsorption temperature (Fig. 10). Yan et al. [23] and Shen et al. [24] studied the adsorption properties of MWCNTs for nitroaromatic compounds and atrazine, respectively, and similar results were also reported. However, the observed positive ΔH° values suggested an endothermic adsorption for 1-naphthylamine and 1-naphthol, which was the reason for the increase in adsorption of 1-naphthylamine and 1-naphthol on as-prepared and oxidized MWCNTs at higher temperature (Fig. 10). Wu [25] and Kuo et al. [26] examined the adsorption efficiency of MWCNTs for reactive dye and direct dyes, respectively, at various temperatures, and the observations obtained in this work agree well with the typical published results.

3.7. Comparison with other adsorbents

A comparison of the Langmuir adsorption capacity (q_{max}) of MWCNTs ($q_{max} = 58.8$ mg/g for 1-naphthylamine, $q_{max} = 54.4$ mg/g for 1-naphthol and $q_{max} = 14.4$ mg/g for phenol) studied in this work with that of other common adsorbents such as natural bentonite ($q_{max} = 18.5$ mg/g for 2-naphthol) [47], apatite ($q_{max} = 9.2$ mg/g for phenol) [48], zeolite ($q_{max} = 4.5$ mg/g for phenol) [49] and kaolinite ($q_{max} = 16.6$ mg/g for Aniline blue dye) [50] documented in the literatures shows that the adsorption capacity of MWCNTs for IACs is higher than that of other adsorbents. Differences in IACs adsorption capacity are associated with the adsorbent physicochemical properties, such as pore structure, functional groups, pH$_{pzc}$ and surface area. Most studies only investigated the adsorption capacity of an adsorbent and few determined the adsorption capacity and related thermodynamics parameters simultaneously. The results observed in this work suggest that the MWCNTs are efficient adsorbent for IACs.

4. Conclusion

In summary, the thermodynamics of IACs adsorption on as-prepared and oxidized MWCNTs were investigated. Based on the results obtained in this work, the following conclusions can be attained:

(1) HNO$_3$-oxidized MWCNTs showed decreased adsorption capacity for 1-naphthylamine, 1-naphthol and phenol compared to that of as-prepared MWCNTs, which might be ascribed to increased electrostatic repulsion, carboxylic groups weakening the π–π interaction and water adsorption.
(2) The equilibrium adsorption of IACs on as-prepared and oxidized MWCNTs at three various temperatures was studied and the adsorption isotherms were described by both Langmuir and Freundlich isotherm models well.
(3) The thermodynamic parameters (ΔH°, ΔS° and ΔG°) of IACs adsorption are calculated for 298, 318 and 338 K, respectively. Generally, the IACs adsorption reactions are considered as spontaneous process because of the negative adsorption standard free energy together with positive standard entropy change.
(4) The observed negative ΔH° values suggested an exothermic adsorption for phenol, while the observed positive ΔH° values suggested an endothermic adsorption for 1-naphthylamine and 1-naphthol.
(5) The as-prepared and oxidized MWCNTs are good adsorbents for the removal of IACs from aqueous solutions. The findings of the present work might have significant implications for the removal of environmental contaminants with as-prepared and oxidized MWCNTs.

References

[1] S. Iijima, Helical microtubules of graphitic carbon, Nature 354 (1991) 56–58.
[2] S. Iijima, T. Ichihashi, Single-shell carbon nanotubes of 1-nm diameter, Nature 363 (1993) 603–605.
[3] N. Jonge, Y. Lamy, K. Schoots, T.H. Oosterkamp, High brightness electron beam from a multi-walled carbon nanotube, Nature 420 (2002) 393–395.

[4] M.S. Dresselhaus, I.L. Thomas, Alternative energy technologies, Nature 414 (2001) 332–337.
[5] M.S. Mauter, M. Elimelech, Environmental applications of carbon-based nano-materials, Environ. Sci. Technol. 42 (2008) 5843–5859.
[6] J. Wang, C. Timchalk, Y. Lin, Carbon nanotube-based electrochemical sensor for assay of salivary cholinesterase enzyme activity: an exposure biomarker of organophosphate pesticides and nerve agents, Environ. Sci. Technol. 42 (2008) 2688–2693.
[7] G.P. Rao, C. Lu, F. Su, Sorption of divalent metal ions from aqueous solution by carbon nanotubes: a review, Sep. Purif. Technol. 58 (2007) 224–231.
[8] B. Pan, B.S. Xing, Adsorption mechanisms of organic chemicals on carbon nan-otubes, Environ. Sci. Technol. 42 (2008) 9005–9013.
[9] C. Lu, H. Chiu, C. Liu, Removal of Zinc(II) from aqueous solution by purified carbon nanotubes: kinetics and equilibrium studies, Ind. Eng. Chem. Res. 45 (2006) 2850–2855.
[10] C. Lu, C. Liu, G.P. Rao, Comparisons of sorbent cost for the removal of Ni^{2+} from aqueous solution by carbon nanotubes and granular activated carbon, J. Hazard. Mater. 151 (2008) 239–246.
[11] C. Lu, Y.L. Chung, K.F. Chang, Adsorption thermodynamic and kinetic studies of trihalomethanes on multiwalled carbon nanotubes, J. Hazard. Mater. B 138 (2006) 304–310.
[12] C. Lu, Y.L. Chung, K.F. Chang, Adsorption of trihalomethanes from water with carbon nanotubes, Water Res. 39 (2005) 1183–1189.
[13] X.J. Peng, Y.H. Li, Z.K. Luan, Z.C. Di, H.Y. Wang, B.H. Tian, Z.P. Jia, Adsorption of 1,2-dichlorobenzene from water to carbon nanotubes, Chem. Phys. Lett. 376 (2003) 154–158.
[14] Q. Liao, J. Sun, L. Gao, The adsorption of resorcinol from water using multi-walled carbon nanotubes, Colloid Surf. A 312 (2008) 160–165.
[15] K. Yang, L. Zhu, B. Xing, Adsorption of polycyclic aromatic hydrocarbons by carbon nanomaterials, Environ. Sci. Technol. 40 (2006) 1855–1861.
[16] K. Yang, X. Wang, L. Zhu, B. Xing, Competitive sorption of polycyclic aro-matic hydrocarbons on carbon nanotubes, Environ. Sci. Technol. 40 (2006) 5804–5810.
[17] K. Yang, B. Xing, Desorption of polycyclic aromatic hydrocarbons from carbon nanomaterials in water, Environ. Pollut. 145 (2007) 529–537.
[18] C.J.M. Chin, L.C. Shih, H.J. Tsai, T.K. Liu, Adsorption of o-xylene and p-xylene from water by SWCNTs, Carbon 45 (2007) 1254–1260.
[19] H.H. Cho, B.A. Smith, J.D. Wnuk, H. Fairbrother, W.P. Ball, Influence of surface oxides on the adsorption of naphthalene onto multiwalled carbon nanotubes, Environ. Sci. Technol. 42 (2008) 2899–2905.
[20] V. Datsyuk, M. Kalyva, K. Papagelis, J. Parthenios, D. Tasis, A. Siokou, I. Kallitsis, C. Galiotis, Chemical oxidation of multiwalled carbon nanotubes, Carbon 46 (2008) 833–840.
[21] K. Laszlo, E.C. Tombacz, Novak, pH-dependent adsorption and desorption of phenol and aniline on basic activated carbon, Colloid Surf. A 306 (2007) 95–101.
[22] W. Chen, L. Duan, L.L. Wang, D.Q. Zhu, Adsorption of hydroxyl- and -substituted aromatics to carbon nanotubes, Environ. Sci. Technol. 42 (2008) 6862–6868.
[23] X.M. Yan, B.Y. Shi, J.J. Lu, C.H. Feng, D.S. Wang, H.X. Tang, Adsorption and des-orption of atrazine on carbon nanotubes, J. Colloid Interface Sci. 321 (2008) 30–38.
[24] X.E. Shen, X.Q. Shan, D.M. Dong, X.Y. Hua, G. Owensc, Kinetics and thermo-dynamics of sorption of nitroaromatic compounds to as-grown and oxidized multiwalled carbon nanotubes, J. Colloid Interface Sci. 330 (2009) 1–8.
[25] C.H. Wu, Adsorption of reactive dye onto carbon nanotubes: equilibrium, kinet-ics and thermodynamics, J. Hazard. Mater. 144 (2007) 93–100.
[26] C.Y. Kuo, C.H. Wu, J.Y. Wu, Adsorption of direct dyes from aqueous solutions carbon nanotubes: determination of equilibrium, kinetics and thermodynamics parameters, J. Colloid Interface Sci. 327 (2008) 308–315.
[27] J.F. Colomer, P. Piedigrosso, I. Willems, C. Journet, P. Bernier, G. van Tendeloo, A. Fonseca, J.B. Nagy, Purification of catalytically produced multi-wall nanotubes, J. Chem. Soc. Faraday Trans. 94 (1998) 3753–3758.
[28] A.G. Rinzler, J. Liu, H. Dai, P. Nikolaev, C.B. Huffman, F.J. Rodriguez-Macias, P.J. Boul, A.H. Lu, D. Heymann, D.T. Colbert, R.S. Lee, J.E. Fischer, A.M. Rao, P.C. Eklund, R.E. Smalley, Large-scale purification of single-wall carbon nanotubes: process, product, and characterization, Appl. Phys. A 67 (1998) 29–37.
[29] D. Aggarwal, M. Goyal, R.C. Bansal, Adsorption of chromium by activated carbon from aqueous solution, Carbon 37 (1999) 1989–1997.
[30] B.L. Chen, E.J. Johnson, B. Chefetz, L.Z. Zhu, B.S. Xing, Sorption of polar and nonpolar aromatic organic contaminants by plant cuticular materials: role of polarity and accessibility, Environ. Sci. Technol. 39 (2005) 6138–6146.
[31] H.P. Boehm, Some aspects of the surface chemistry of carbon blacks and other carbons, Carbon 32 (1994) 759–769.
[32] C.S. Lu, F.S. Su, S. Hu, Surface modification of carbon nanotubes for enhancing BTEX adsorption from aqueous solutions, Appl. Surf. Sci. 254 (2008) 7035–7041.
[33] W. Chen, L. Duan, D. Zhu, Adsorption of polar and nonpolar organic chemicals to carbon nanotubes, Environ. Sci. Technol. 24 (2007) 8295–8300.
[34] C.L. Chen, X.K. Wang, Adsorption of Ni(II) from aqueous solution using oxidized multiwall carbon nanotubes, Ind. Eng. Chem. Res. 45 (2006) 9144–9149.
[35] I. Langmuir, The adsorption of gases on plane surfaces of glass, mica and plat-inum, J. Am. Chem. Soc. 40 (1918) 1361–1403.
[36] M. Kilpatrick, L.L. Baker Jr., C.D. McKinney Jr., Studies of fast reactions which evolve gases. The reaction of sodium–potassium alloy with water in the pres-ence and absence of oxygen, J. Phys. Chem. 57 (1953) 385–390.
[37] B. Pan, B.S. Xing, W.X. Liu, S. Tao, X.M. Lin, Y.X. Zhang, H.S. Yuan, H.C. Dai, X.M. Zhang, Y. Xiao, Two-compartment sorption of phenanthrene on eight soils with various organic carbon contents, J. Environ. Sci. Health Part B 41 (2006) 1333–1347.
[38] C. Lu, H. Chiu, Chemical modification of multiwalled carbon nanotubes for sorption of Zn^{2+} from aqueous solution, Chem. Eng. J. 139 (2008) 462–468.
[39] S. Kang, M. Mauter, M. Elimelech, Physicochemical determinants of multi-walled carbon nanotube bacterial cytotoxicity, Environ. Sci. Technol. 42 (2008) 7528–7534.
[40] D.H. Lin, B.S. Xing, Adsorption of phenolic compounds by carbon nanotubes: role of aromaticity and substitution of hydroxyl groups, Environ. Sci. Technol. 42 (2008) 7254–7259.
[41] K. Yang, W. Wu, Q. Jing, L. Zhu, Aqueous adsorption of aniline, phenol, and their substitutes by multi-walled carbon nanotubes, Environ. Sci. Technol. 42 (2008) 7931–7936.
[42] J. Chen, M.A. Hamon, H. Hu, Y. Chen, A.M. Rao, P.C. Eklund, R.C. Haddon, Solution properties of single-walled carbon nanotubes, Science 282 (1998) 95–98.
[43] M. Franz, H.A. Arafat, N.G. Pinto, Effect of chemical surface heterogeneity on the adsorption mechanism of dissolved aromatics on activated carbon, Carbon 38 (2000) 1807–1819.
[44] D.Q. Zhu, J.J. Pignatello, Characterization of aromatic compound sorptive inter-actions with black carbon (charcoal) assisted by graphite as a model, Environ. Sci. Technol. 39 (2005) 2033–2041.
[45] R.W. Coughlin, F.S. Ezra, Role of surface acidity in the adsorption of organic pollutants on the surface of carbon, Environ. Sci. Technol. 2 (1968) 291–297.
[46] A.S. Gnihotri, M. Rostam-Abadi, M.J. Rood, Temporal changes in nitrogen adsorption properties of single-walled carbon nanotubes, Carbon 42 (2004) 2699–2710.
[47] J. Wei, R. Zhu, J. Zhu, F. Ge, P. Yuan, H. He, C. Ming, Simultaneous sorption of crystal violet and 2-naphthol to bentonite with different CECs, J. Hazard. Mater. 166 (2009) 195–199.
[48] A. Bahdod, S. El Asri, A. Saoiabi, T. Coradin, A. Laghzizil, Adsorption of phenol from an aqueous solution by selected apatite adsorbents: kinetic process and impact of the surface properties, Water Res. 43 (2009) 313–318.
[49] R.I. Yousef, B. El-eswed, The effect of pH on the adsorption of phenol and chlorophenols onto natural zeolite, Colloid Surf. A 334 (2009) 92–99.
[50] E.I. Unuabonaha, K.O. Adebowale, F.A. Dawodu, Equilibrium, kinetic and sorber design studies on the adsorption of Aniline blue dye by sodium tetraborate-modified Kaolinite clay adsorbent, J. Hazard. Mater. 157 (2008) 397–409.